

New insights on the quantum-classical division in light of Collapse Models

Fernanda Torres*

*Department of Physics, University of Houston, Houston, Texas 77024-5005, USA and
Facultad de Ciencias - CUICBAS, Universidad de Colima, Colima, C.P. 28045, México*

Sujoy K. Modak[†] and Alfredo Aranda[‡]

Facultad de Ciencias - CUICBAS, Universidad de Colima, Colima, C.P. 28045, México

We argue, in light of Collapse Model interpretation of quantum theory, that the fundamental division between the quantum and classical behaviors might be analogous to the division of thermodynamic phases. A specific relationship between the collapse parameter (λ) and the collapse length scale (r_C) plays the role of the coexistence curve in usual thermodynamic phase diagrams. We further claim that our functional relationship between λ and r_C is strongly supported by the existing International Germanium Experiment (IGEX) collaboration data. This result is preceded by a self-contained discussion of quantum measurement theory and the Ghirardi-Rimini-Weber (GRW) model applied to the free wavepacket dynamics.

Quantum mechanics (QM) persists in providing opportunities for interpretations and understanding. Among the questions that keep us interested are the “measurement problem” and the issue of the inter-phase between classical and quantum phenomena, i.e. when could one say firmly that a distinction between the two occur?, where is the boundary? Although as old as QM itself, these interesting questions remain subject to investigation and can lead to (have led to) interesting ideas. In this letter we explore a particular setting – within the realm of so-called Collapse Models [1]-[6] – and make a case that identifying and classifying quantum and classical “phases” might be similar to the identification and classification of phases in the thermodynamic/magnetic/QGP systems.

“Measurement problem” is explicit when we treat an apparatus quantum mechanically to explain the outcome of a measurement. We inevitably land in an unbreakable Von-Neumann chain (VNC) for which Collapse Models [1]-[6] come to the rescue. To see that consider A to be the apparatus that measures a system S having an observable \mathcal{O} . Then, the time evolution of the system-apparatus is controlled by a linear unitary operator U , whose evolution conserves the conjugation relations, and is given by,

$$U|\psi_0\rangle|A_0\rangle = \sum_n c_n |\psi_n\rangle|A_n\rangle. \quad (1)$$

The initial state of the system is $|\psi_0\rangle$ and of the apparatus is $|A_0\rangle$. Time evolution makes a linear superposition of the $S + A$ system due to the use of the unitary operator U which, in turn, invites some troubles. First the eventual appearance of a statistical mixture of states originating from the system and the apparatus after the measurement is performed. But even to get to the statistical mixture invites a second problem: the information about the entire system ($S + A$) during the measurement process is not complete. It is necessary to have another apparatus B that can measure the final state of the ap-

paratus A in order to know the final state of $S + A$. In this way, cumulatively, we end up with a measurement process in a VNC where finally some conscious mind (observer) is needed to determine a stopping point to break it. Thus observer becomes an inseparable part of a physical theory!

In order to break the VNC *spontaneously*, collapse models [1]-[6] add stochasticity along with the linear Schrödinger evolution, working in a way that microscopic quantum behavior is practically preserved, but importantly, macroscopic superpositions are effectively suppressed assuring that the macroscopic wave functions are well localized in space.

Treating the system S and apparatus A quantum mechanically, initially one associates S in a state $|\psi_0\rangle$ and A in a well-localized state $|A_0\rangle$. Without loss of generality, one can set the pointer’s position (signalling the center of mass position of A) at zero and assuming A is static its momentum is also zero. Initially there is no interaction between the system and the apparatus. The complete system is $S + A$, and the total Hamiltonian is given by $H = H_A + H_{int}$ where $H_A = P^2/2M$ refers to the Hamiltonian of the apparatus of mass M when treated as a free particle. Also, there is an interaction between the apparatus and the system given by H_{int} . Due to the smallness of the quantum system we can neglect the free Hamiltonian of the system S for simplicity. The interaction between the S and A can be modelled in the following way [7]:

$$H_{int} = \frac{d\beta}{dt} f(\mathcal{O})P \quad (2)$$

where $d\beta/dt$ is the change of the interaction during the interval (t_0, t_1) . $\beta(t)$ vanishes for $t \leq t_0$, then increases from t_0 to t_1 , and at some later time $t \geq t_1$ becomes one. Thus the interaction Hamiltonian is zero before t_0 and after t_1 . In this model details of the interaction between the system and the apparatus are unspecified but the overall consequence of such a process is contemplated.

The operator $f(\mathcal{O})$ is a function of the observable to be measured which, from a dimensional analysis, has a dimension of length. Once an interaction begins, the $S + A$ system evolves in the following manner:

$$\begin{aligned} |\Phi(t)\rangle &= e^{-\frac{i}{\hbar} \int H dt} |\psi_0\rangle |A_0\rangle \\ &= \sum_n c_n e^{-\frac{i}{\hbar} H_A t} e^{-\frac{i}{\hbar} \beta(t) f(\mathcal{O}_n) P} |\psi_n\rangle |A_0\rangle \\ &= \sum_n c_n |\psi_n\rangle |A_n(t)\rangle. \end{aligned} \quad (3)$$

The above equation is truly applicable for the interval $[t_0, t_1]$ and it indicates that the system and apparatus are in an entangled state; that is, the eigenstate $|\psi_n\rangle$ of the system is entangled with the eigenstate of the apparatus, given by

$$|A_n(t)\rangle = e^{-\frac{i}{\hbar} H_A t} e^{-\frac{i}{\hbar} \beta(t) f(\mathcal{O}_n) P} |A_0\rangle. \quad (4)$$

Therefore the whole $S + A$ system is now in a superposition of states and due to entanglement when, in the apparatus space, the pointer picks an eigenstate $|A_n\rangle$, the above superposition in (3) ceases to exist making the system collapse to its eigenstate $|\psi_n\rangle$. There are however two issues that need to be sorted out in order to mimic a true quantum mechanical measurement: (i) it is necessary to recover stochastic nature of the collapse process and the Born probability rule on the selection of eigenstates of the system, and (ii) it is important to ensure that apparatus eigenstates $|A_n\rangle$ can be macroscopically separated even if the system eigenstates $|\psi_n\rangle$ are not.

The first requirement can be fulfilled by interpreting $\beta(t)$ as a white noise function for the simplest case. This stochastically selects the eigenvalues $f(\mathcal{O}_n)$ dictating the apparatus pointer positions (i.e., associated pointer eigenstates $|A_n\rangle$). Therefore, entanglement between S and A will then ensure that the eigenvalues \mathcal{O}_n (or the system eigenstates $|\psi_n\rangle$) are obtained likewise, and therefore the Born probability rule is ensured. In order to explain how the second requirement is fulfilled let us consider a schematic diagram in Fig. 1 summarizing the mathematical arguments of [7]. The system space includes possible states of the system with corresponding eigenvalues ($|\psi_n, \mathcal{O}_n\rangle$) which are entangled with the apparatus eigenstates and corresponding position space eigenvalues ($|A_n, f(\mathcal{O}_n)\rangle$). The position of the pointer in the apparatus space is represented by $Q = \langle Q \rangle$ which has an uncertainty ΔQ before and after measurements. Depending on the noise term $\beta(t)$, the expectation value of the pointer's position may be found in the vicinity of $f(\mathcal{O}_n)$ such that the uncertainty $\Delta Q \ll f(\mathcal{O}_n)$, or an identical situation with another outcome $f(\mathcal{O}_m)$ such that the uncertainty $\Delta Q \ll f(\mathcal{O}_m)$. When the above situation is contemplated we say the measurements have returned eigenvalues \mathcal{O}_n and \mathcal{O}_m provided the distance between the two pointer positions are macroscopic, i.e.,

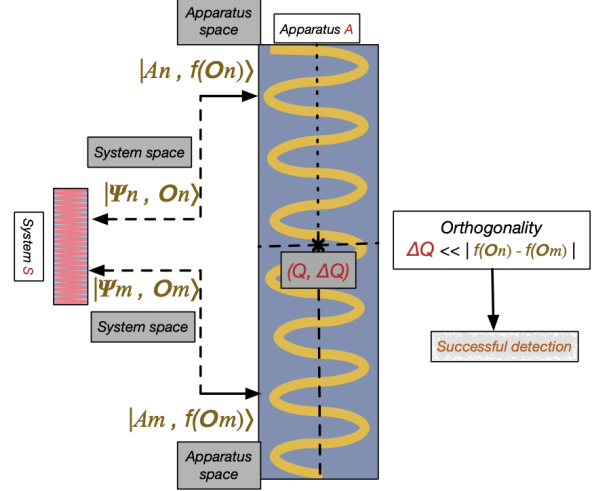


FIG. 1. Schematic diagram describing the idea of quantum theory of measurement, following Benatti, Ghirardi, Rimini and Weber [7], considering both the system S and apparatus A quantum mechanically. For details see text.

$\Delta Q \ll |f(\mathcal{O}_m) - f(\mathcal{O}_n)|$, which is also a necessary combination for $|A_n\rangle$ s to form a basis [7]. A collective explanation in terms of the density matrix is the following: before the wavepacket reduction the statistical operator is

$$\rho = \sum_{m,n} c_n c_m^* |\psi_m\rangle \langle \psi_n| \otimes |A_m\rangle \langle A_n| \quad (5)$$

and when the measurement is performed the pointer state $\langle Q \rangle$ is found near a specific $f(\mathcal{O}_n)$ and ΔQ is far small as stated above, which will imply that the apparatus state is collapsed to $|A_n\rangle$ to a sufficient accuracy and thus the density operator above will be diagonal

$$\rho = \sum_n |c_n|^2 |\psi_n\rangle \langle \psi_n| \otimes |A_n\rangle \langle A_n|. \quad (6)$$

When such a diagonalization takes place we interpret this as the reduction of the wavepacket and, in doing so, the initial pure density operator evolves into a proper mixture [8] as required by a measurement.

The Ghirardi-Rimini-Weber (GRW) version [2] considers “measurement like effects” happen discretely in time following a Poisson distribution with or without measurement and as an integral part of the quantum dynamics. A parameter λ is introduced as the mean frequency of such discrete collapse events. Once again, the reduction of the wavepacket is represented by the diagonalization of the density operator, which when collapse happens suffers a jump $\rho \rightarrow T_q[\rho]$ in the vicinity of q [2, 7] such that

$$T_q[\rho] = \sqrt{\frac{\alpha}{\pi}} \int_{\mathbb{R}} dx e^{-\frac{\alpha}{2}(q-x)^2} \rho e^{-\frac{\alpha}{2}(q-x)^2}, \quad (7)$$

and α provides the second important parameter – the collapse length scale $r_C = 1/\sqrt{\alpha}$. The length r_C has the following role – if initially two given states $|\psi_1\rangle$ and $|\psi_2\rangle$ (making the density operator) are individually localized in region less than r_C while the distance between them is more than r_C , we consider them distinct states and truly in superposition. The density matrix constructed by them is initially pure and satisfies the modified Schrödinger evolution,

$$\frac{d\rho}{dt} = -\frac{i}{\hbar}[H, \rho] + \lambda(T_q[\rho] - \rho). \quad (8)$$

By virtue of the above equation it takes a time equivalent to $1/\lambda$ for the initial pure density operator to become diagonal or mixed. Note that, the above equation (8) can be easily generalized for N particle systems by scaling λ to $N\lambda$ [2, 7].

For a free wavepacket (8) becomes

$$\begin{aligned} \frac{\partial}{\partial t} \langle q' | \rho(t) | q'' \rangle &= \frac{i\hbar}{2m} \left(\frac{\partial^2}{\partial q'^2} - \frac{\partial^2}{\partial q''^2} \right) \langle q' | \rho(t) | q'' \rangle \\ &\quad - \lambda(1 - e^{-(\alpha/4)(q' - q'')^2}) \langle q' | \rho(t) | q'' \rangle. \end{aligned} \quad (9)$$

The above differential equation can be rigorously solved [2, 7] to yield

$$\begin{aligned} \langle q' | \rho(t) | q'' \rangle &= \frac{1}{2\pi\hbar} \int_{-\infty}^{\infty} dk \int_{-\infty}^{\infty} dy e^{-(i/\hbar)ky} \\ &\quad \times F(\lambda, k, q' - q'', t) \langle q' + y | \rho_S(t) | q'' + y \rangle, \end{aligned}$$

where

$$F(\lambda, k, q, t) = e^{-\lambda t \left(1 - \frac{1}{t} \int_0^t d\tau e^{-(\alpha/4)(q - k\tau/m)^2} \right)} \quad (10)$$

is the term driving the nonlinear dynamics of state reduction and the $\rho_S(t)$ is defined in the Schrödinger picture. At an initial time $t = 0$, $F(\lambda, k, q, t) = 1$ and there is no distinction from the standard Schrödinger initial value. However, at any later time we have a modified dynamics which is influenced by the occasional collapse processes for the ensemble of identically prepared initial free wavepackets. Following [2] one can calculate expectation values of various observables such as position, momentum and their functions by derivating the function defined in (10). Up to the quadratic order of operator expectation values, one obtains [2]

$$\langle \hat{q} \rangle_{GRW} = \langle \hat{q} \rangle_S \quad (11)$$

$$\langle \hat{q}^2 \rangle_{GRW} = \langle \hat{q}^2 \rangle_S + \frac{\alpha\lambda\hbar^2}{6m^2} t^3 \quad (12)$$

$$\langle \hat{p} \rangle_{GRW} = \langle \hat{p} \rangle_S \quad (13)$$

$$\langle \hat{p}^2 \rangle_{GRW} = \langle \hat{p}^2 \rangle_S + \frac{\alpha\lambda\hbar^2}{2} t \quad (14)$$

$$\langle \hat{q}\hat{p} \rangle_{GRW} = \langle \hat{q}\hat{p} \rangle_S + \frac{\alpha\lambda\hbar^2}{4m} t^2. \quad (15)$$

In the remaining part of this work we show remarkable usefulness of above results not only for constraining Collapse Models but also for the general understanding on the quantum-classical division.

First recall the law of free wavepacket expansion due to the uncertainty principle in the standard Schrödinger picture. The square of the width $\xi_S = \Delta q_S^2 = \langle q^2 \rangle_S - \langle q \rangle_S^2$ satisfies the following second order equation [9],

$$\frac{d^2}{dt^2} \xi = \frac{2\varpi_0}{m^2}, \quad (16)$$

where $\varpi_0 = \langle p_0^2 \rangle_S - \langle p_0 \rangle_S^2$ is the initial variance in momentum space which for the free wavepacket remain constant over time. By integrating twice one gets the time evolution of the width of the wavepacket,

$$\Delta q_S(t) = \sqrt{\Delta q_{0,S}^2 + \dot{\xi}_{0,S} t + \frac{\Delta p_{0,S}^2}{m^2} t^2} \quad (17)$$

where the subscript zero means the quantity is evaluated at the initial time $t = 0$ (in Schrödinger picture). The initial value of the time derivative of the variance satisfies $\dot{\xi}_{0,S} = \frac{1}{m} [-i\hbar + 2(\langle qp \rangle_{0,S} - \langle q \rangle_{0,S} \langle p \rangle_{0,S})]$ which is related with the initial correlation between the position and momentum of the wavepacket. For a Gaussian shaped wavepacket one can show that this derivative term vanishes altogether [9]. We now express the standard formula (17) in the GRW picture by using the set of equations (11)-(15). Since the Collapse Model only influences average values dynamically with time, initial values remain unchanged. Defining $\Delta q_{GRW} = \sqrt{\langle \hat{q}^2 \rangle_{GRW} - \langle \hat{q} \rangle_{GRW}^2}$, and using (11)-(15) we have the following expansion formula for the width of a free wavepacket in the GRW picture,

$$\Delta q_{GRW}(t) = \sqrt{\Delta q_{0,S}^2 + \dot{\xi}_{0,S} t + \frac{\Delta p_{0,S}^2}{m^2} t^2 + \frac{\alpha\lambda\hbar^2}{6m^2} t^3}. \quad (18)$$

We see that the initial values remain unchanged and we get a new term, in addition to the standard Schrödinger expansion rate, cubic in time and contributing to an accelerated expansion. Considering once again a Gaussian shape one has a vanishing derivative term and saturation for the uncertainty principle $\Delta p_0 \Delta q_0 = \hbar/2$. Using this we can express (18) completely in the position space,

$$\Delta q_{GRW}(t) = \sqrt{\Delta q_{0,S}^2 + \frac{\hbar^2}{4m^2 \Delta q_{0,S}^2} t^2 + \frac{\alpha\lambda\hbar^2}{6m^2} t^3}. \quad (19)$$

The above equation is quite extraordinary – a single equation bearing the classical, quantum and collapse effects. Setting $\hbar = 0$ would turn off both the quantum and collapse contributions signalling, once again, that the noise corresponding to the collapse parameter λ is purely quantum. On the other hand, by setting $\lambda = 0$ we just

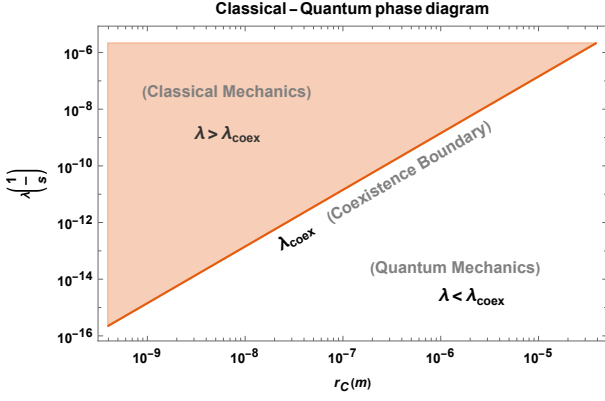


FIG. 2. Unconstrained log-log plot showing the classical and quantum phases for the relevant $\lambda - r_C$ plane. We set $t = 10^{17}$, a characteristic value considering the age of the universe in (20). The plot is closely analogous to the coexistence curve in thermodynamic phase diagram. For details see the text.

turn of the collapse effect and thereby end up with conventional quantum result. It is interesting to see that a direct effect of collapses of wavefunctions in fact increases the rate of expansion the wavepacket. This is expected due the “kicks” generated by occasional collapses of the wavefunctions constructing the wavepacket itself.

To compare the strength of collapse mechanism to the standard quantum effect we define the Collapse-to-Quantum Ratio (CQR),

$$\varrho(t; \alpha, \lambda) = \frac{2}{3}(\alpha \lambda \Delta q_{0,S}^2) t \quad (20)$$

Replacing α by the collapse length scale r_C we can express

$$\varrho(t; r_C, \lambda) = \left(\frac{2\lambda \Delta q_{0,S}^2}{3r_C^2} \right) t. \quad (21)$$

To give an estimate consider a characteristic value for the collapse length scale $r_C = 10^{-7} \text{ m}$ and for hydrogen $\Delta q_0^2 \simeq 10^{-20} \text{ m}^2$. Thus for the free Hydrogen molecular wavepacket

$$\varrho(t; \alpha, \lambda) = \frac{2 \times 10^{-6} \lambda t}{3}. \quad (22)$$

Note, however, that original GRW arguments based on macro and micro domains set a very wide bound for the collapse parameter [2], $10^{-16} \leq \lambda \leq 10^7$, which has obviously been constrained by various experiments (as summarized in the Fig. 4 of [10]).

Here we show how to constrain λ from our discussion of the free wavepacket dynamics. The argument is quite simple: Hydrogen is abundantly found in the universe and has been the main source of energy of stars for billions of years. This stability for a free Hydrogen atom is possible only if the collapse term is subdominant

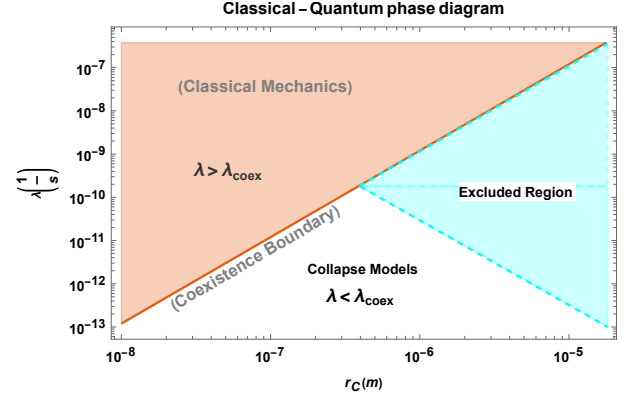


FIG. 3. Log-log plot showing the classical mechanics and Collapse Model parameter spaces in the $\lambda - r_C$ plane for mass-proportional collapse model. The functional relationship resulting λ_{coex} line is experimentally supported by the IGEX data [10, 20]. The parameter space of the phase diagram in Fig. 2 is reduced after implementing other useful bounds summarized in Fig. 4 of [10]. For details see the text.

(to the standard quantum mechanical term) even for a timescale comparable to the age of the universe. That is, for ($t \sim 10^{17} \text{ s}$), we can safely assume that CQR is below unity for Hydrogen and using (22) we get,

$$\varrho(t = 10^{17}; \alpha = 10^{10}, \lambda) \leq 1 \implies \lambda \leq 1.5 \times 10^{-11}.$$

Thus from a very general consideration, we can constrain the collapse parameter to an unprecedented narrow band given by $10^{-16} \leq \lambda \leq 10^{-11}$. Now given the fact that the collapse length scale r_C can vary from the mesoscopic to near microscopic values, there exist a range of possible values for r_C given by $10^{-8} \text{ m} \leq r_C \leq 10^{-4.5} \text{ m}$. By virtue of (21) we can generate corresponding bounds on λ by using the fact that $\varrho \leq 1$. The very definition of CQR in (21) provides us a guiding principle for distinguishing classical and quantum systems in light of the Collapse Models. Since CQR tracks the strength of collapse dynamics in comparison with the standard quantum dynamics, we can interpret that for a system to be considered “quantum” we must have $\varrho < 1$ and violation of the same will imply a system as “classical”. Therefore, $\varrho = 1$ will provide a boundary curve, very similar to a coexistence curve in the phase diagram of thermodynamic systems. For our consideration of Hydrogen atoms originated in the early universe, $\varrho_{\text{coex}} = 1$ in (21) provides a curve $\lambda_{\text{coex}} = (1.5 \times 10^3) r_C^2$ which is plotted in Fig. 2 for the allowed range of r_C mentioned before.

Now we compare our theoretical estimates with the experimental data. A nice summary of various bounds is plotted in $\lambda - r_C$ plane in [10]. They come from variety of experiments started with the LISA Pathfinder data [11, 12], Cantilever based experiments [13], ultra-cold layered forced sensors [14], Gravitational-Wave detectors [15], assuming effective collapse rate at the meso-

scopic scale [16] and the data from International Germanium experiment (IGEX) [17–20]. Although some of these experiments used so called the continuous version of GRW model, the parameter space for (r_C, λ) remains very close as in the discrete GRW, and therefore for all practical purposes we can compare our bound with the results summarized [10].

Using the definition of CQR in (20) one derives $\lambda \propto r_C^2$ for an arbitrary but fixed time t . This functional dependence, plotted as the coexisting boundary λ_{coex} in Fig. 2, is extraordinarily supported by the X-ray emission data collected by the IGEX experiment [17–20] (summarized in blue dotted line of Fig. 4 in [10]). This match can also be made numerically accurate with one arbitrariness – one can match both the mass-proportional and non-mass-proportional collapse models considered in [20] by suitably adjusting the time t when the CQR $\varrho \geq 1$. For the mass-proportional collapse model and considering a Gaussian distribution for the data Piscicchia *et al.* [20] estimate $\lambda_{m,p} \leq 8.1 \times 10^{-12}$ (for $r_C = 10^{-7}\text{m}$). Here, in Fig. 2, we can easily translate the bound on λ arising from (20) with that in the mass-proportional collapse model [6] simply by using the relationship $\lambda_{m,p} = \lambda \left(\frac{m_H}{m_n} \right) = 2\lambda$ where m_H is the mass of a Hydrogen atom and m_n of a nucleon. Replacing λ by $\lambda_{m,p}$ in (20) we can reproduce the bound $\lambda_{m,p} \leq 8.1 \times 10^{-12}$ by setting $t \geq 3.70 \times 10^{17}\text{s}$, which is of the order of the age of the universe. This tells us mass-proportional collapse models cannot be discarded as yet. On the other hand we can also reproduce the non-mass-proportional bound of [20] 2.4×10^{-18} by using our original definition of CQR in (20) and by setting $t \geq 6.25 \times 10^{23}$. Irrespective of the numerical values, physically these inequalities give us an estimate as to when the collapse dynamics start dominating the quantum dynamics on a free particle. In mass proportional model this time is in the hindsight while for non-mass proportional model this time is still 6 orders of magnitude away. This arbitrariness cannot be fixed within our framework, but if experimental evidence prefers one collapse model over the other, then we know exactly when collapse effect will dominate over the quantum effect for a free particle. If we chose the mass-proportional model and other bounds exhibited in Fig. 4 of [10] we can further constrain the Classical-Quantum phase diagram in Fig. (2) which is represented in Fig. (3).

Authors thank Paolo Amore and Saurya Das for their valuable feedback on the pre-print. Research of FT and SKM are supported by SEP-CONACyT research grant CB/2017-18/A1S-33440, Mexico.

* mftorrescabrera@uh.edu

† smodak@uocol.mx

‡ fefo@uocol.mx

- [1] P. Pearle, *Reduction of the state vector by a nonlinear Schrödinger equation*, Phys. Rev. D 13, 857 (1976)
- [2] G.C. Ghirardi, A. Rimini and T. Weber, *Unified dynamics for microscopic and macroscopic systems*, Phys. Rev. D 34, 470 (1986).
- [3] G.C. Ghirardi, P. Pearle and A. Rimini, *Markov processes in Hilbert space and continuous spontaneous localization of systems of identical particles*, Phys. Rev. A 42, 78 (1990).
- [4] A. Bassi and G.C. Ghirardi, *Dynamical reduction models*, Phys. Rept. 379, 257 (2003).
- [5] S.L. Adler and A. Bassi, , Science 325, 275 (2009).
- [6] A. Bassi, K. Lochan, S. Satin, T. P. Singh and H. Ulbricht, *Models of Wave-function Collapse, Underlying Theories, and Experimental Tests*, Rev. Mod. Phys. **85**, 471-527 (2013)
- [7] F. Benatti, G. C. Ghirardi, A. Rimini, & T. Weber, *Quantum mechanics with spontaneous localization and the quantum theory of measurement*, Nuovo Cimento B, 100(1), 27–41 (1987).
- [8] B. d’Espagnat, *Conceptual Foundations of Quantum Mechanics*, (Addison-Wesley, 2nd. ed., 1976)
- [9] A. Messiah, *Quantum Mechanics*, North-Holland Publishing, 1961 (Ch. VI, pp. 216-222).
- [10] A. Vinante, M. Carlesso, M., A. Bassi et al., *Narrowing the Parameter Space of Collapse Models with Ultracold Layered Force Sensors*, Physical Review Letters, 125, 100404 (2020).
- [11] M. Armano et al, *Beyond the Required LISA Free-Fall Performance: New LISA Pathfinder Results down to 20 μHz* , Physical Review Letters, 120, 061101 (2018).
- [12] M. Carlesso, M. Paternostro, H. Ulbricht, A. Vinante, & A. Bassi, *Non-interferometric test of the continuous spontaneous localization model based on rotational optomechanics*, New Journal of Physics, 20, 083022 (2018).
- [13] A. Vinante, R. Mezzena, P. Falferi, M. Carlesso, & A. Bassi, *Improved Noninterferometric Test of Collapse Models Using Ultracold Cantilevers*. Phys. Rev. Lett. 119, 110401 (2017).
- [14] F. Laloe, W. J. Mullin, & P. Pearle, *Heating of trapped ultracold atoms by collapse dynamics*, Phys. Rev. A 90, 052119 (2014).
- [15] Matteo Carlesso, Angelo Bassi, Paolo Falferi, and Andrea Vinante, *Experimental bounds on collapse models from gravitational wave detectors* Physical Review D, 94, 124036 (2016).
- [16] S. L. Adler, *Lower and Upper Bounds on CSL Parameters from Latent Image Formation and IGM Heating*, J. Phys. A 40, 2935 (2007).
- [17] H. S. Miley, F. T. Avignone, III, R. L. Brodzinski, J. I. Collar, and J. H. Reeves, *Suggestive evidence for the two-neutrino double-beta decay of Ge-76*, Physical Review Letters 65, 3092 (1990).
- [18] C. E. Aalseth et al., *Neutrinoless double- β decay of ^{76}Ge : First results from the International Germanium Experiment (IGEX) with six isotopically enriched detectors*, Physical Review C, 59, 2108 (1999).
- [19] Collett, B., Pearle, P., Avignone, F., & Nussinov, S. (1995). *Constraint on collapse models by limit on spontaneous x-ray emission in Ge*, Foundations of Physics, 25(10), 1399–1412.
- [20] K. Piscicchia et al, *CSL Collapse Model Mapped with the Spontaneous Radiation*, Entropy, 19(7), 319 (2017).